Activation for Cell Fusion in *Chlamydomonas:* Analysis of Wild-type Gametes and Nonfusing Mutants

URSULA W. GOODENOUGH, PATRICIA A. DETMERS, and CAROL HWANG
Department of Biology, Washington University, St. Louis, Missouri 63130

ABSTRACT Gametes of *Chlamydomonas reinhardi* become activated for cell fusion as the consequence of sexual adhesion between membranes of mating-type *plus* and *minus* flagella. By using tannic acid plus *en bloc* uranyl acetate staining, and by fixing at very early stages in the mating reaction, we have demonstrated the following. (*a*) Activation of the *minus* mating structure entails major modifications in the structure of the organelle, causing it to double in size and to concentrate surface coat material, termed fringe, into a central zone. (*b*) The unactivated *plus* mating structure is endowed with fringe that moves with the tip of the actin-filled fertilization tubule during activation. Pre-fusion images suggest the occurrence of a specific recognition event between the *plus* and *minus* fringes. (*c*) Gametes carrying the *imp-1* mutation fail to form a fringe and are unable to fuse. The *imp-1* mutation is linked to the mating-type *plus* (mt^+) locus, suggesting that the gene specifying the synthesis or insertion of fringe is encoded in this sector of the genome. (*d*) Gametes carrying the *imp-11* mutation fail to form both a normal fringe and a normal submembranous density beneath the fringe, and are also unable to fuse. The *imp-11* mutation converted a wild-type *minus* cell into a pseudo-*plus* strain; a model to explain this conversion proposes that the normal *imp-11* gene product represses *plus*-specific genes concerned with *Chlamydomonas* gametogenesis.

Biological membranes do not ordinarily fuse with one another: the eucaryotic cell is filled with membrane systems and organelles that maintain their integrity. The important exceptions to this rule include endocytosis, the rough endoplasmic reticulum (RER) → Golgi → exocytosis transit, the fertilization of gametes, and the formation of such syncytia as myofibrils. In each case, the relevant membranes fuse in a highly specific fashion, and only in response to well defined physiological signals (e.g. receptor clustering, Ca^{++} fluxes, or–possibly–the presence of a clathrin coat).

Fusion between gametic cells of *Chlamydomonas reinhardi* (reviewed in references 8 and 9) is particularly well suited to experimental analysis. (*a*) The discrete sector of the plasma membrane that is specialized for this event can be readily identified in either thin section or freeze-fracture replicas (2, 7, 13, 23, 24). (*b*) Fusion specificity resides in this membrane sector: mating-type *plus* (mt^+) gametes will fuse only with minus (mt^-) partners of the same species. (*c*) These membranes acquire the capacity to fuse in response to a defined physiological signal, namely, the adhesion of flagellar membranes (1, 12, 18, 22, 25). (*d*) *Chlamydomonas* can be readily manipulated genetically (4, 20), offering the possibility of isolating nonfusing mutants.

Previous studies from this laboratory (13, 24) defined several stages in the acquisition of fusion capacity. The present report exploits the ability of fixation in the presence of tannic acid and *en bloc* staining with uranyl acetate to reveal new features of the activation process that occur moments after flagellar adhesion. We also describe the properties of two mutant strains, specifically defective in their ability to fuse, whose fusogenic membrane sectors are unmistakably mutant in phenotype. These strains are particularly interesting in that one carries a mutation linked to mt^+; the other arose via an $mt^- \rightarrow$ pseudo-*plus* mutation. We proposed, therefore, that the mating-type locus exerts direct control over fusion specificity.

MATERIALS AND METHODS

Gametes were harvested from week-old plates into nitrogen-free minimal medium (NF) as described (16), and their mating efficiencies assessed by a light-microscope scoring procedure (18).

Mutagenesis was performed by irradiating vegetative wild-type mt^- (wt^-) cells with UV, and nonmating mutants were detected by their inability to form zygotes with *arg-2* mt^+ gametes; details of these protocols are given in reference 10. For reversion analysis, a culture of *imp-11* vegetative cells was divided into six separate aliquots to avoid scoring a reverted clone more than once. Each aliquot was irradiated to a 90% kill level and placed in the dark for 18 h to prevent photoreactivation. The cells were then allowed to differentiate into

THE JOURNAL OF CELL BIOLOGY · VOLUME 92 FEBRUARY 1982 378-386

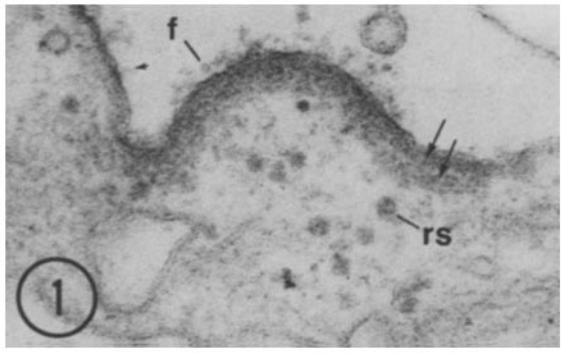

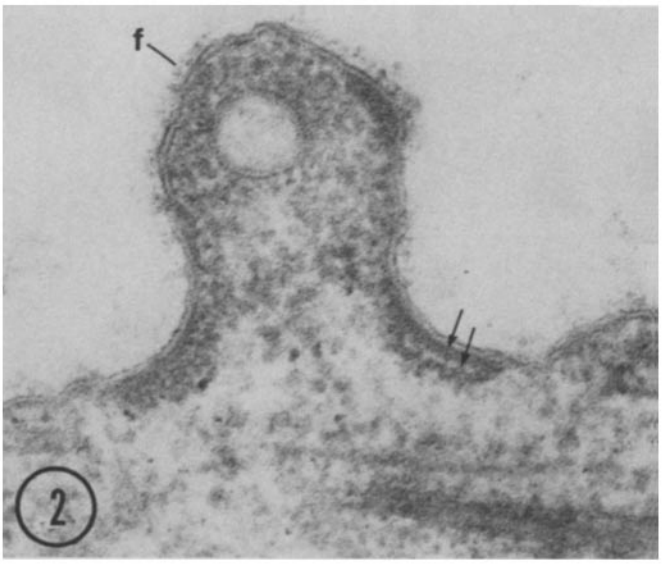

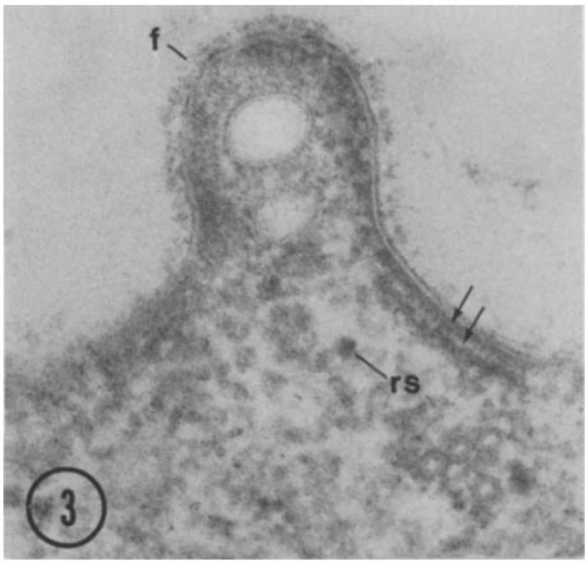

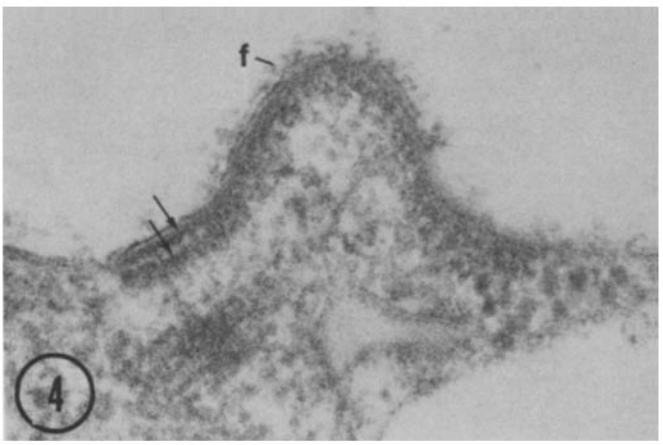

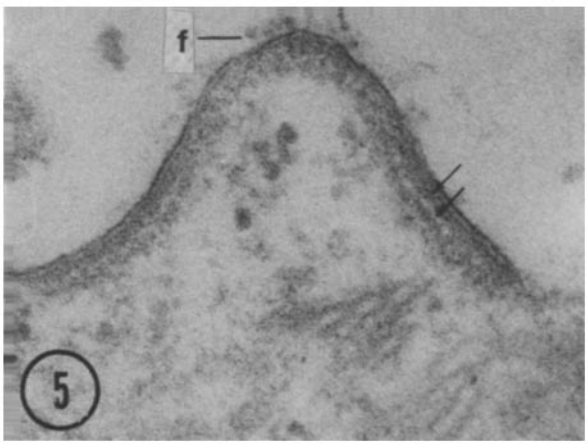

FIGURE 1 Unactivated wt$^-$ mating structure. The plasma membrane is underlain by a band of dense material, the membrane zone, which appears bipartite (double arrows) at the periphery. The membrane surface is covered with a layer of projections termed fringe (*f*), which is visibly more dense and prominent than the occasional wisps associated with the contiguous plasma membrane (arrowhead). *rs*, ribosome. × 118,000.

FIGURE 2 Bud stage of wt$^-$ mating-structure activation elicited by 2 min of flagellar agglutination with the nonfusing mutant *imp-1*. The bipartite sector of the membrane zone (double arrows) lies at the base of the bud. The bud interior contains a membrane vesicle, particulate material, and patches of submembranous dense material. The surface fringe (*f*) is discontinuous, being absent, for example, from a sector of membrane at the apical end of the bud. × 118,000.

FIGURE 3 Bud stage of wt$^-$ mating-structure activation as in Fig. 2. Submembranous dense material covers a larger portion of the bud membrane but is still discontinuous, for example, to the left of the bud apex. The fringe (*f*) is now continuous and very uniform in length. *rs*, ribosome; double arrows, bipartite zone. × 118,000.

FIGURE 4 Fully activated wt$^-$ mating structure from a 2-min agglutination with the nonfusing mutant *imp-11*. Some particulate material remains in the interior but the structure has converted from a bud to a dome-shaped structure and has a smaller surface area. The fringe (*f*) is concentrated over the continuous layer of submembranous dense material, the central zone; the fringe-free bipartite sectors of the original membrane zone (double arrows) lie on either side. × 118,000.

FIGURE 5 Fully activated wt$^-$ mating structure from a 2-min mixture with the *imp-1* mutant. Particulate material is absent so that the organelle interior resembles that of the unactivated mating structure (Fig. 1). Fringe (*f*) is concentrated at the apical portion of the central zone; bipartite region at double arrows. × 118,000.

gametes in NF. Half of each culture was mixed with *arg-2 mt*$^+$ gametes; the other half was mixed with *arg-2 mt*$^-$ gametes. The mating mixtures were plated onto arginine-free minimal medium (10) to minimize the growth of unmated gametes, and the plates were stored in the dark for at least a week to promote zygote maturation. The plates were then exposed to chloroform vapor for 30 s to kill any surviving unmated gametes, and were placed in the light to allow zygote germination and mitosis. The few colonies present on each plate were subcloned, and the mating types of their constituent cells were determined by test mating with wt$^+$ and wt$^-$.

For electron microscopy, gametes or mating mixtures were suspended in 6 ml of NF at a density of 1.5×10^7 cells/ml. To this, 1.5 ml of 4% glutaraldehyde (Ladd Research Industries, Inc., Burlington, Vt.) and 1% tannic acid (Mallinckrodt Inc., St. Louis, Mo.) in NF was added in successive 0.1 ml drops, with rapid agitation between drops. After a 30-min fixation at room temperature, the cells were pelleted by gentle centrifugation, washed in NF, suspended in cold 0.5% OsO_4 (Fisher Scientific Co., Pittsburgh, Pa.) in 0.1 M sodium phosphate buffer, pH 6.0 for 20–45 min, washed in water, *en bloc* stained in 1% aqueous uranyl acetate for 20 min at room temperature, and dehydrated and embedded as described (15). Stained sections were examined with an Hitachi HU-11C or a JEOL 100CX electron microscope. Measurements of mating structures were made on electron micrographs with a map reader.

RESULTS

The Unactivated wt$^-$ Mating Structure

Fig. 1 illustrates the wt$^-$ mating structure in an unmated gamete viewed in cross section. As previously described (2, 6, 13, 23, 24), this organelle consists of a curved dense layer, the membrane zone, which lies beneath the plasma membrane to one side of the basal-body complex. The organelle is cup-shaped in three dimensions (24) so that longitudinal cross sections generate images of various sizes; to compare with later stages, however, we measured 12 unactivated organelles and obtained a mean length of 422 nm with a standard deviation of 43 nm. A wt$^-$ clone used in a previous study (24), it should be noted, possessed much smaller mating structures (340 nm average), and we have noted similar strain-specific size differences in other cases.

The combination of glutaraldehyde fixation with tannic acid (TA) and *en bloc* staining with uranyl acetate (UA) brings out a layer of fuzzy material (Fig. 1*f*) overlying the central portion of the membrane surface. Though the contiguous plasma membrane ocassionally displays fuzzy wisps (Fig. 1, arrowhead), such a dense regular coat is unique to the membrane surface of the mating structure, and we therefore propose the term **fringe** to designate this material.

Mating Structure Activation in wt$^-$

Dramatic changes occur in the morphology of the mating structure when wt$^-$ gametes are allowed to undergo sexual flagellar agglutination and are then fixed with TA and treated with UA. These changes are most readily documented when wt$^-$ gametes are mixed with *plus* mutant strains that are unable to fuse (see below), because activation and fusion are normally so closely coupled; however, occasional images of the sort reported here have been captured during wt$^-$ × wt$^+$ matings as well.

Figs. 2–5 show four representative electron micrographs of activating wt$^-$ mating structures. All were obtained from samples fixed after 2 min of agglutination; however, mating structures with the prominent budded appearance (Figs. 2 and 3) are found only in samples fixed during the first few minutes after agglutination, whereas mating structures with the domed appearance (Figs. 4 and 5) persist in samples where agglutination has continued for longer periods. We therefore conclude that the budded mating structures convert into the domed mating structures and that Figs. 2–5 present a temporal sequence of events.

BUDDED STAGE: Figs. 2 and 3 illustrate the first detectable response of the wt$^-$ mating structure to flagellar agglutination: a prominent bud forms with a total surface length of ~1,000 nm. The original material of the membrane zone is located at the base of each bud. Whereas this material is vaguely bipartite in unactivated organelles (Fig. 1, double arrows), it becomes prominently so after activation (Figs. 2–5, double arrows). Measurements of these two bipartite "halves" give a summed mean length of 367 nm ± 48 (SD). Because the mean length of the unactivated organelle is 422 nm, some 45 nm of the unactivated structure may be included in the bud. The buds, however, contain an additional 600 nm of membrane which, we proposed, is added during the activation process.

The bud interior typically contains 1–2 small vesicles; whether these participiate in bud formation or are fortuitous inclusions cannot be decided from the static images. A very regular layer of extracellular coat material associates with the bud membrane; this appears discontinuous in Fig. 2 and continuous in Fig. 3. Because fringe is no longer associated with the bipartite material at the base, it seems likely that at least some of this coat is composed of the original fringe found associated with unactivated organelles; whether additional fringe components are added during activation or whether preexisting components are redistributed cannot be decided. The bud interior is filled with particulate material, much smaller than ribosomes (c.f. Fig. 1 and 3, *rs*), which is not seen anywhere in the vicinity of unactivated mating structures. Patchy submembranous densities are also visible in the bud, and images such as Fig. 2 suggest that the particulate material may condense against the cytoplasmic face of the membrane to form these patches.

DOMED STAGE: Figs. 4 and 5 show what we interpret to be fully activated organelles. The bipartite regions at the base have dimensions comparable to those of bipartite "halves" of the bud. The central region has again transformed, however: it is now less prominent than the bud and measures only ~400 nm rather than 600 nm. It bears a continuous dense fringe (*f*) on its surface which is often concentrated in an apical tuft (Fig. 5), and it is underlain by a homogeneous layer of dense material, hereafter denoted the central zone, rather than the discontinuous patches seen in the bud. The particulate matter which filled the bud also diminishes in prominence (Fig. 4) and finally disappears altogether (Fig. 5). Indeed, comparison of the fully activated mating structure (Fig. 5) with its unactivated counterpart (Fig. 1) shows that the two are superficially similar in morphology but that the activated organelle has increased in size by a factor of two and carries a more distinct bipartite differentiation.

The wt$^+$ Mating Structure

The mating structure of the unmated wt$^+$ gamete differs from its wt$^-$ counterpart in three ways. (*a*) It is larger and more oblate in shape (6, 24), with a mean cross-section surface length of 520 nm ± 105 nm (SD). (*b*) Its surface fringe (*f*) is far more prominent and dense than the wt$^-$ fringe (compare Figs. 6 and 7 with Fig. 1), so that it can be seen very faintly even without TA/UA treatment (24). (*c*) It possesses a broad doublet zone (Figs. 6 and 7, *dz*) beneath its membrane zone. The doublet zone, we should note, is distinctly different from the bipartite region of the wt$^-$ mating structure: the doublet zone is itself bipartite so that three layers are present when it is apposed to the membrane zone (Fig. 6, triple arrows) rather than the two

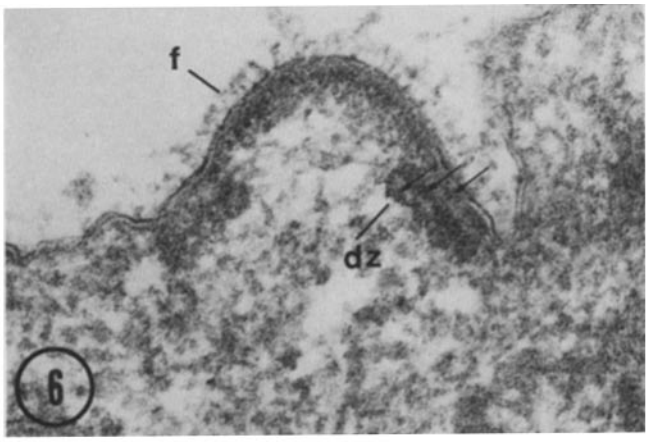

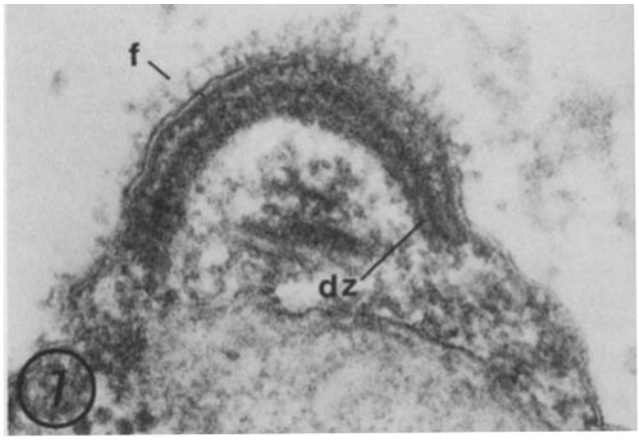

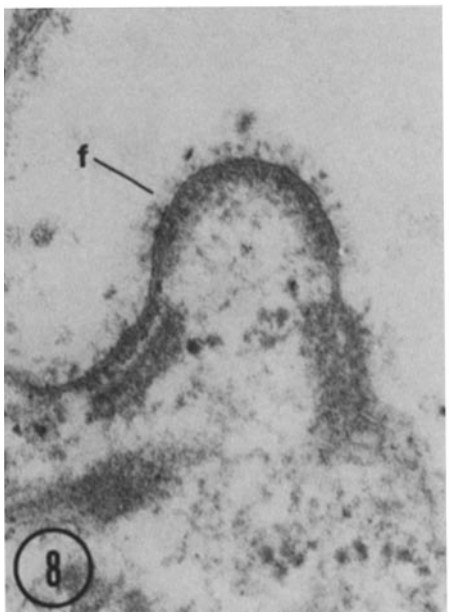

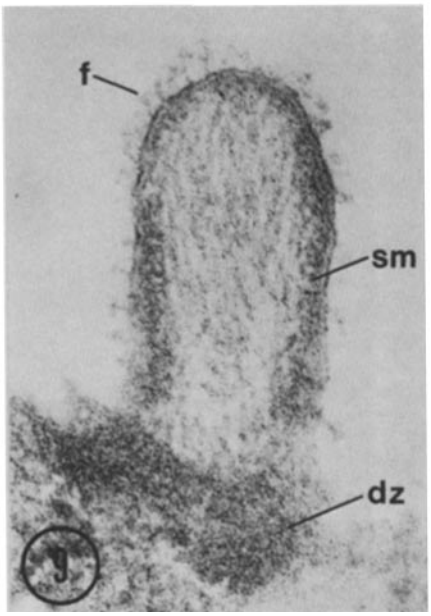

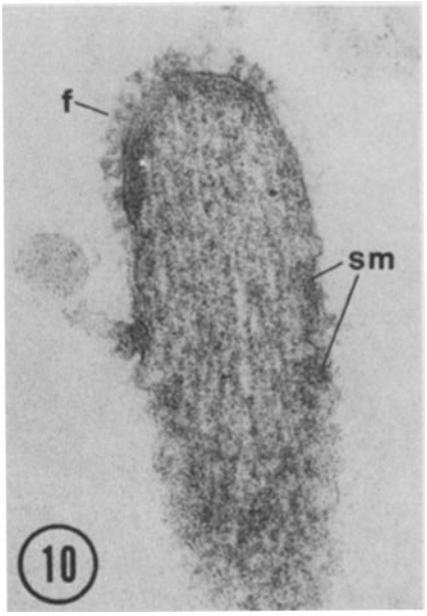

FIGURES 6 and 7 Unactivated wt^+ mating structures. The plasma membrane is underlain by a band of dense material, the membrane zone. Beneath this is the wide doublet zone (*dz*), whose medial discontinuity is included in the Fig. 6 section. The three layers that form when the doublet zone underlies the membrane zone are indicated by the triple arrows. Fringe (*f*) covers the whole surface of the organelle and is longer and more luxurient than the wt^- fringe. × 118,000.

FIGURE 8 Bud stage of wt^+ mating structure activation elicited by a 5-min agglutination with isolated wt^- flagella (24). The sector of the membrane zone overlying the doublet-zone discontinuity has lifted into a bud, carrying with it most of the surface fringe (*f*). × 118,000.

FIGURE 9 Early wt^+ fertilization tubule, elicited by a 5-min agglutination with wt^- in the presence of 25 μM EDTA, which prevents cell fusion. Actin filaments extend from the doublet zone (*dz*) cut in tangential section. A long stretch of submembranous material (*sm*) associates with both sides of the new membrane in the fertilization tubule, and fuzz projects from its surface. The fringe (*f*) is located at the tip of the fertilization tubule overlying what appears to be the original membrane zone material, an area somewhat narrower and more delicate than the lateral strips of submembranous density. × 118,000.

FIGURE 10 Elongated wt^+ fertilization-tubule, elicited by a 2-min agglutination with wt^- gametes, showing the distal portion of a 1.5-μm actin-filled projection. The submembranous material (*sm*) is now in discontinuous lateral patches, but the membrane zone and associated fringe (*f*) remains continuous at the tip. × 118,000.

layers seen in wt^- structures (Figs. 1–5, double arrows); moreover, the doublet zone bears a small medial discontinuity (7) which may (Fig. 6) or may not (Fig. 7) be included in cross section, whereas the bipartite region invariably displays a medial discontinuity (Figs. 1–5).

Activation of the wt^+ mating structure begins with the formation of a bud (13) (Fig. 8). The bud then fills with longitudinally arrayed actin filaments (3) that appear to polymerize from a nucleation site in the doublet zone (Fig. 9, *dz*), converting the bud into a fertilization tubule (Fig. 10); only the tip of a fertilization tubule is shown in Fig. 10, but serial sections show this particular tubule to extend 1.5 μm from the cell surface. In both the bud and the fertilization tubule, submembranous material associates with the lateral membranes; this material is continuous in the bud (Fig. 9, *sm*) and discontinuous in the fertilization tubule (Fig. 10, *sm*), and it is often overlain by wisps of surface fuzz (Fig. 9). The fringe, however, clearly remains associated with the tips of both the bud and the tubule (Figs. 8–10*f*). This cap of fringe, moreover, measures ~300 nm, which is the approximate length of the fringe associated

with the membrane that overlies the medial discontinuity in the unactivated mating structure (Fig. 1). We propose, therefore, that the original fringe and its underlying membrane zone move out with the tip of the elongating fertilization tubule, and that additional membrane is somehow added to the sides.

Pre-Fusion Fringe Interactions

Fig. 11 shows the usual image of *Chlamydomonas* gametic fusion: the tip of the fertilization tubule has already fused with the wt^- mating structure, and the dense regions marking the fusion sites (arrows) are most uninformative; one cannot tell whether they derive from the wt^+ tip, the wt^- central zone, or the wt^- membrane zone. Despite exhaustive serial sectioning, we have yet to view any images of pre-fusion contacts in normal mating mixtures, suggesting that fusion occurs extremely rapidly.

A most informative image has, however, been obtained under experimental conditions wherein wt^- gametes were pretreated with 400 μM cytochalasin D and then mixed with untreated wt^- partners in the presence of the drug. As seen in Fig. 12, the drug has prevented actin polymerization but not elongation of the wt^- mating structure into a pseudo-fertilization tubule (3). The tip of this pseudo-tubule has made contact with an activated wt^- mating structure, and the drug has interfered with or slowed down the fusion process sufficiently to permit a view of the interacting membranes. It is clear that contact is highly localized to the two regions of fringe. The original bipartite membrane-zone region of the wt^- organelle (Fig. 12, double arrows) takes no apparent part in the interaction, nor does the membrane that lines the sides of the pseudo-tubule. It is not known whether the drug elicits the flattening of the tubule tip to make maximal contact with the central zone or whether such flattening occurs normally. The image suggests, however, that the two fringe regions adhere specifically to one another.

The imp-1 Mating Structure

The *imp-1* mutation, which maps to the *mt*$^+$ locus on Linkage Group VI (4), was originally described as causing a defect in microfilament polymerization (13): gametes fixed after 1 h of agglutination showed no evidence that the *imp-1* mating structures had undergone outgrowth of the fertilization tubule. Reexamination of the mutant fixed after only several minutes of agglutination shows this interpretation to be in error: actin-

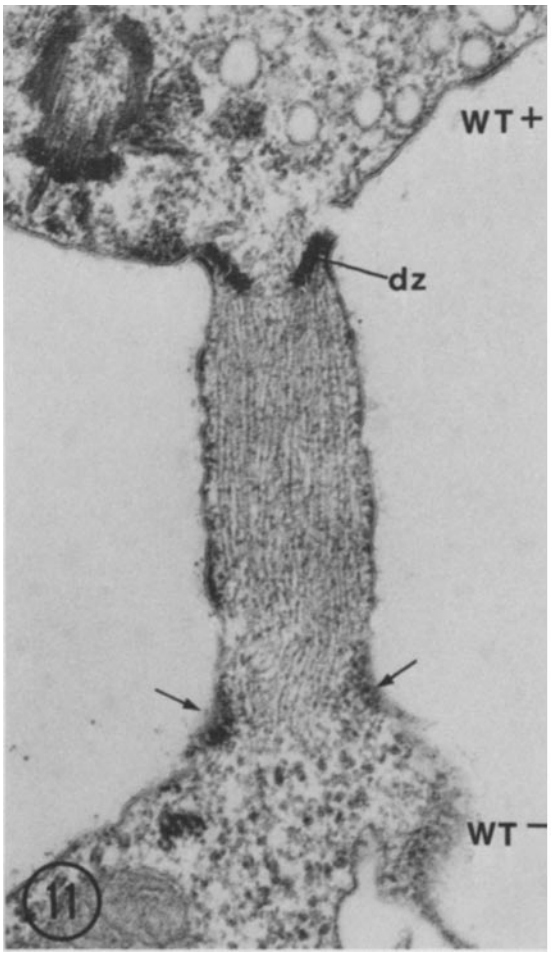

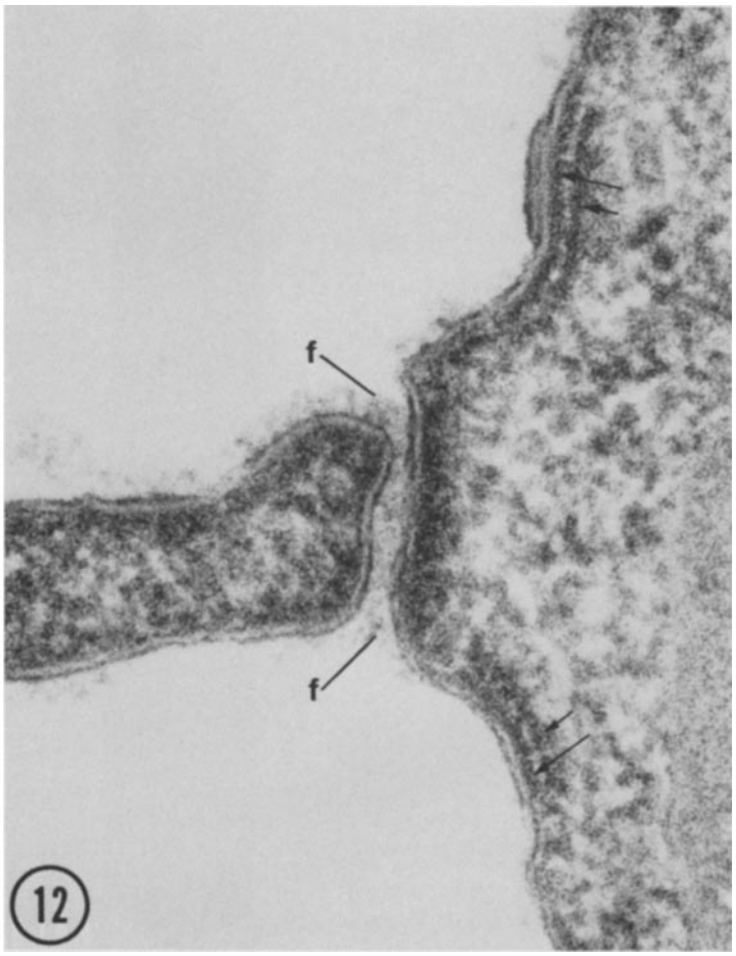

FIGURE 11 Cytoplasmic bridge between wt^+ (upper) and wt^- (lower) gametes. The doublet zone (*dz*) marks the wt^+ end of the bridge. Fusion has occurred in the region marked by the two arrows. The dense material in the fusion zone is most likely a hybrid of wt^+ membrane zone and wt^- central zone. × 60,000.

FIGURE 12 Pre-fusion interaction between tip of wt^+ fertilization tubule (left) and activated wt^- mating structure (right), whose bipartite membrane-zone sectors are marked by the sets of double arrows. The fertilization tubule contains no actin because cytochalasin D was present in the mating mixture. The surface fringes (*f*) of the fertilization tubule and the wt^- central zone are enmeshed along a broad flattened region of contact. × 195,000.

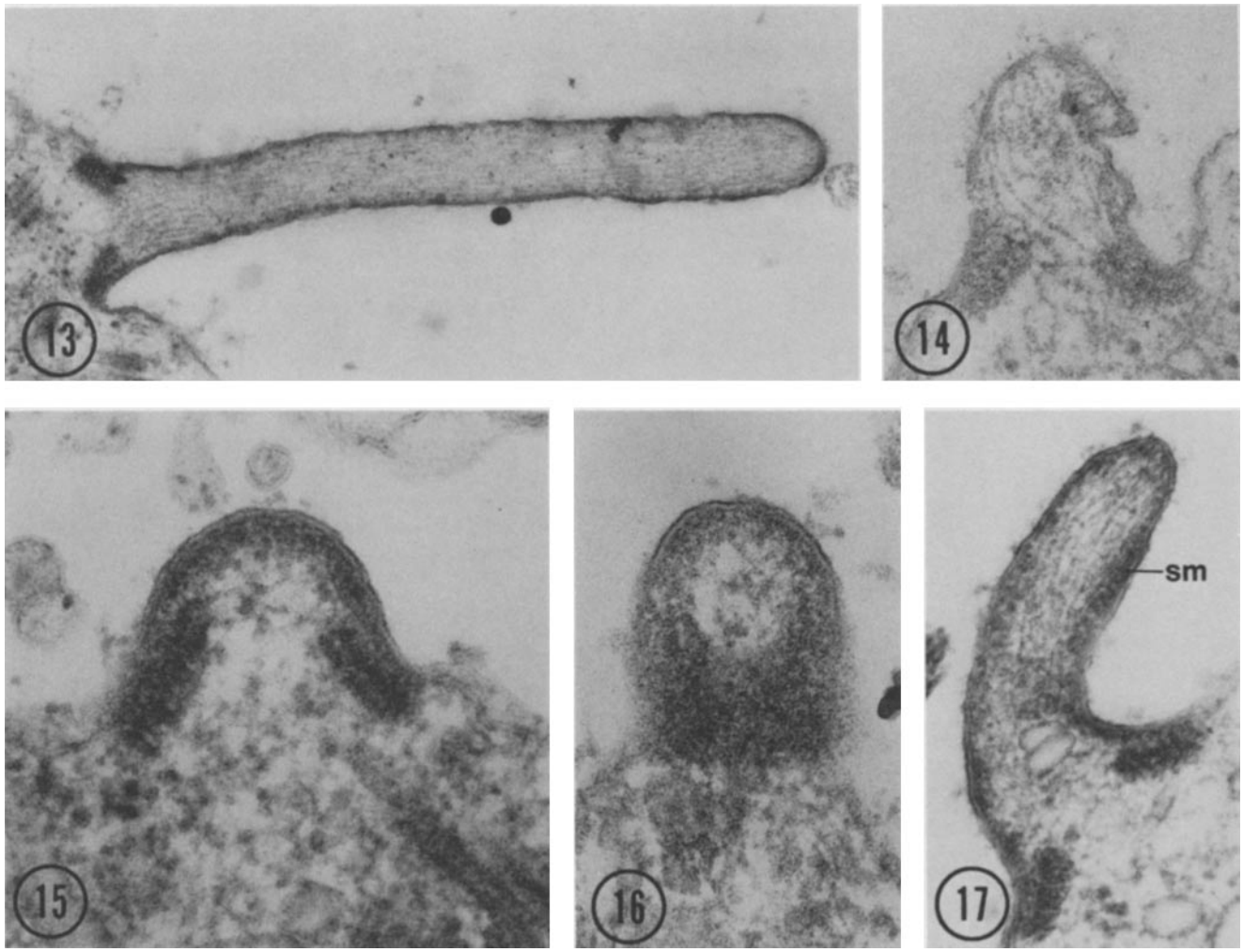

FIGURE 13 Elongated *imp-1 mt*$^+$ fertilization tubule erected 2 min after mixing with wt$^-$ gametes. Normal actin polymerization and tubule outgrowth have occurred, but no fringe is evident at the apex. × 60,000.

FIGURE 14 Collapsed *imp-1 mt*$^+$ fertilization tubule in a gamete mixed with wt$^-$ gametes for 30 min. The actin filaments are bent and disorganized, and the membrane is distorted. × 118,000.

FIGURE 15 and 16 Two *imp-1 mt*$^+$ unactivated mating structures shown in central medial and in tangential section. The surface membrane is without fringe (compare with Figs. 6 and 7). × 118,000.

FIGURE 17 Early *imp-1* fertilization tubule. As with the comparable wt$^+$ structure (Fig. 9), the sides of the tubule acquire a continuous zone of submembranous material (*sm*), and occasional fuzz projects from the lateral membrane surface. A dense regular fringe is absent from the tip. × 94,000.

filled fertilization tubules grow out normally (Fig. 13), but after 30 min they lose their rigidity and collapse (Fig. 14), eventually reassuming the unactivated morphology described in the original report (13).

Despite their ability to activate fertilization tubules, *imp-1* gametes are only very rarely able to fuse with wt$^-$ gametes (10), suggesting that some other feature of their mating structures is defective. Examination of unactivated *imp-1* mating structures after TA/UA treatment shows that whereas an apparently normal membrane zone is present, the amount of fringe material is drastically reduced (Figs. 15 and 16). Activation is accompanied by the normal addition of dense material along the sides of the bud and tubule (Fig. 17), but a cap of fringe and its underlying membrane zone are not detectable at the end of the tubule (Figs. 13 and 17). We propose, therefore, that this defect accounts for the inability to fuse.

The imp-11 Mating Structure

Fig. 18 shows an unactivated *imp-11* mating structure; stages in activation are shown in Figs. 19 and 20. The membrane zone, at best, carries scattered fuzz, but no dense fringe can be seen. Submembranous material associates with the membranes of the bud and fertilization tubule (Figs. 19 and 20, *sm*), but the tips again carry only sparse fuzz and no underlying membrane zone (compare Figs. 19 and 20 with Figs. 8 and 9).

The *imp-11* mutant is even less likely to fuse than is *imp-1*. Whereas *imp-1* is sufficiently leaky to have yielded a few zygotes for genetic analysis (10), repeated attempts to isolate rare zygotes after *imp-11* × wt$^-$ (or *imp-11* × wt$^+$) matings have been completely unsuccessful. Because *imp-11* has more apparent fringe than *imp-1*, but fuses less well, it is possible that the fringe displayed by *imp-11* is nonfunctional, having perhaps

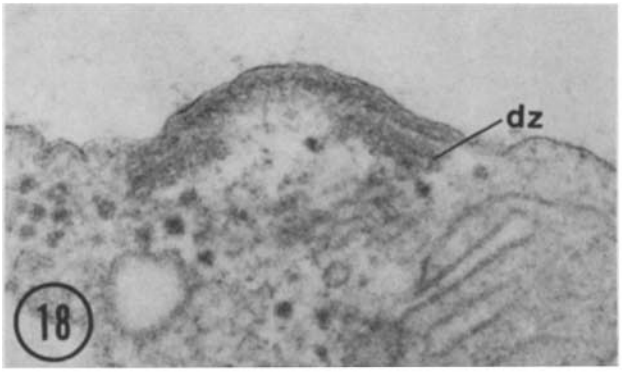

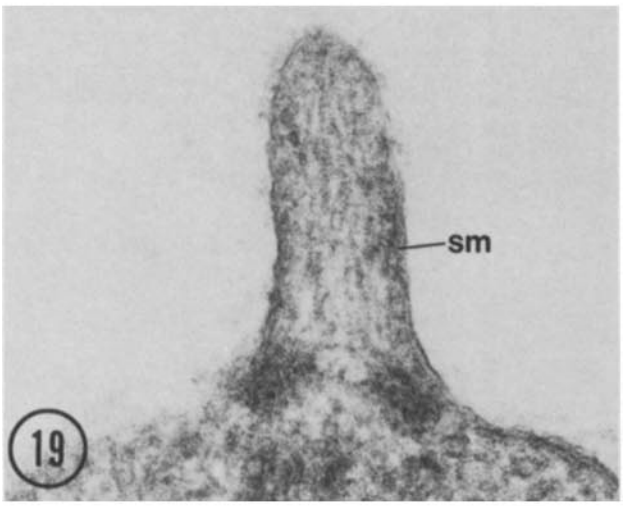

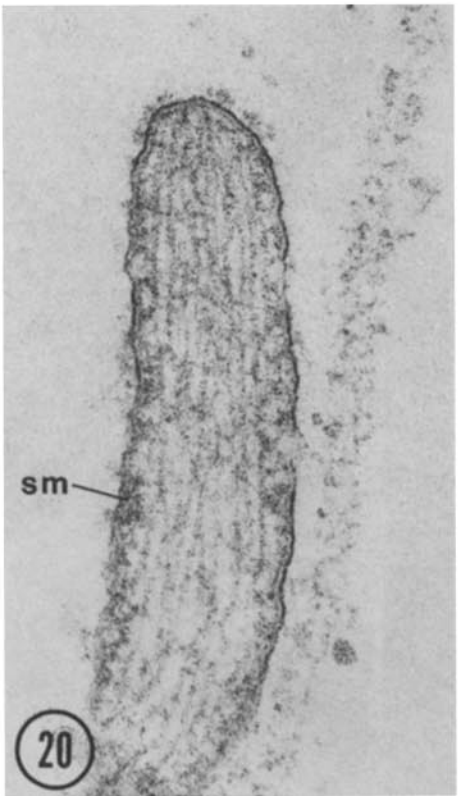

FIGURE 18 Unactivated *imp-11* mating structure. The membrane zone and underlying doublet zone (*dz*) are like wt$^+$, but the surface membrane bears only a few wisps of fuzz, no organized fringe (compare with Figs. 6 and 7). × 118,000.

an inappropriate chemical composition. It is also possible that the apparent absence of a normal membrane zone at the tip of the *imp-11* fertilization tubule, in combination with its sparse fringe, accounts for the nonleaky phenotype.

The Origin of imp-11

Except for its mutant membrane zone, the *imp-11* gamete has all the properties of a normal *mt*$^+$ cell: it agglutinates avidly with wt$^-$ gametic flagella, and possesses an apparently normal doublet zone and ability to polymerize actin (Figs. 18–20). The strain is of considerable interest, therefore, in that it derives from mutagenesis of a wt$^-$ culture. It can, moreover, revert to wt$^-$: in six independent tests in which a total of 10^6 UV survivors were screened for reversion as described in Materials and Methods, at least one *minus* revertant was present in three of the samples, giving a reversion rate of $\sim 3 \times 10^{-6}$. The revertants behave like wt$^-$ cells by all criteria available. In these same experiments, no mutations converted *imp-11* to normal, fusing wt$^+$ cells. The implications of these findings are considered in the Discussion.

DISCUSSION

Activation of the wt$^-$ Mating Structure

Two features of the wt$^-$ mating structure are described in this report. First, the combination of fixation in the presence of tannic acid and *en bloc* staining with uranyl acetate allows visualization of a surface coat or fringe overlying the surface membrane, more modest than its wt$^+$ counterpart but distributed in a comparable fashion. Second, fixation at early timepoints reveals an intermediate bud stage in the wt$^-$ response to flagellar agglutination.

The membrane surface length of the bud is 2–3 times that of the original mating structure, and surface coat material is associated with this additional membrane. Fig. 21 diagrams two alternate sources for the additional membrane. In the exocytic model drawn in Fig. 21*a*, novel membrane is imported to the site of the mating structure in the form of cytoplasmic vesicles and is inserted into its medial aspect to form the central zone. In the membrane-flow model drawn in Fig. 21*b*, the membrane originally overlying the mating structure becomes pushed out to form the central zone of the bud and is replaced by plasma membrane that flows in from the periphery. The two models have distinct implications. The idea that new, fusogenic (?) fringe material is added to the mating structure at the time of activation is more readily explained by the first model, and comparison of Figs. 2–5 with Fig. 1 suggests that activated structures carry additional fringe. The origin of the central cluster of intramembrane particles in activated wt$^-$ mating structures (24) is also more readily explained by an insertion model. However, considerable rearrangement of existing materials might occur during a protrusion/flow event, and the issue clearly cannot be settled by thin-section analysis.

FIGURE 19 Early *imp-11* fertilization tubule. Actin polymerization is normal, but the endowment of lateral submembranous material (*sm*) is much sparser than in either *imp-1* (Fig. 17) or wt$^+$ (Fig. 9). No discrete membrane zone is located at the tip, and the surface fuzz lacks the dense regular morphology of normal fringe. × 118,000.

FIGURE 20 Elongated *imp-11* fertilization tubule, showing distal half. Patchy submembranous material (*sm*) is seen along the sides, but the tip bears no membrane zone (compare with Fig. 10), and its surface coat is short and sparse. × 118,000.

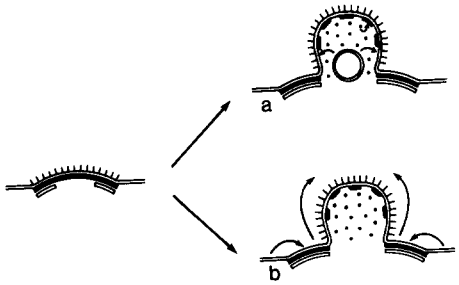

FIGURE 21 Alternate models of membrane addition to the wt⁻ bud: (*a*) Exocytosis; (*b*) Membrane flow. Arrows indicate direction of membrane movement. See text for details.

Gametic Fusion

Our results suggest that *Chlamydomonas* cell fusion is a two-step event: recognition and, perhaps, adhesion occur between the fringe regions first (Fig. 12), and membrane fusion itself follows. That the fringe material plays a key role is strongly suggested by the inability of the mutant lacking fringe, *imp-1*, to undergo cell fusion. The role of the underlying membrane-zone material is less certain. The *imp-11* mutant clearly has a defective membrane zone that fails to move with the tip of the fertilization tubule; however, its endowment of fringe also appears abnormal, being shorter and sparser than that of wt⁺. Therefore, the inability of this mutant strain to fuse may also be explained by defective fringe.

The necessity for a membrane-recognition step in *Chlamydomonas* cell fusion is evident from an independent line of investigation. We have noted (12) that when wt⁺ cells are stimulated to activate their mating structures by being presented with wt⁻ flagella or antiflagellar antibody, millions of cells with erect fertilization tubules are closely apposed, yet fusion does not occur. Fusion also fails to occur in analogous experiments with activated wt⁻ gametes. Apparently, therefore, activated mating structures are primed to undergo a *plus-minus* recognition/adhesion event between *plus* and *minus* membranes, which we propose is mediated by fringe interactions, and this event, in turn, leads to the poorly understood process of membrane fusion.

We should point out that fusions mediated by the paramyxoviruses, such as Sendai virus, have features parallel to those described here. The elegant studies of Choppin and collaborators (19) have shown that the viral coat first binds to appropriate membrane surface ligands and then initiates fusion via its F protein.

It is intriguing to speculate that the fringe material coating the wt⁺ mating structure is identical to the *plus* agglutinin present on the flagellar membrane surface, and that the wt⁻ fringe is the same as the *minus* agglutinin. In other words, one model would propose that *Chlamydomonas* uses the same biochemical system for two independent recognition and adhesion events. This model does not easily explain the phenotypes of existing mutant strains, however: *sag mt*⁺ mutants that have no flagellar agglutinin can nonetheless mate normally if their fertilization tubules are artificially activated (12); conversely, the fusion-defective mutants described here have functional flagellar agglutinins. Therefore, we presently prefer the alternate model, namely, that *Chlamydomonas* specifies two sets of complementary recognition systems that are biochemically different. The two models can be critically tested by immunocytochemistry using monoclonal antibody probes against flagellar agglutinin molecules; the relevant hybridomas are presently being generated in this laboratory.

The imp-11 Mutation

Because the *imp-11* strain is nonconditionally sterile, its genetic analysis will require polyethylene glycol-mediated cell fusion (17), which is currently in progress. Meanwhile, the *imp-11* phenotype gives several insights into the genetic specification of gametic traits in *Chlamydomonas*.

It is known from previous studies that genes involved in the sexual differentiation of *Chlamydomonas* fall into two classes. Some are directly linked to the *mt* locus itself (10, 20), so that certain genes will be found exclusively in *mt*⁺ but not *mt*⁻ cells, and vice-versa. Others are carried by both haploid mating types but are limited in their expression to one or the other type (5, 6, 11, 14); thus, for example, the "sex-limited" *sag-1* locus (11) functions to specify *plus* flagellar agglutinability in haploid *mt*⁺ cells, but is apparently not expressed in haploid *mt*⁻ cells. Because the haploid *imp-11* mutant derives from wt⁻ and can readily revert to wt⁻, we can assume that it carries an *mt*⁻ but not an *mt*⁺ locus and can write its genotype as *imp-11 mt*⁻.

Our current hypothesis is that the gene marked by the *imp-11* mutation normally functions to repress the expression of *plus*-specific sex-limited genes in wt⁻ gametes. This hypothesis predicts that the *imp-11 mt*⁻ mutant will express *plus*-specific sex-limited genes, but it should not be able to express any genes carried within the absent *mt*⁺ locus. Therefore, the fact that *imp-11* gametes express *plus* agglutinins and *plus* mating structures is most simply explained by proposing that these traits are specified by sex-limited genes (e.g. the *sag-1* locus). The fact that *imp-11* gametes fail to develop a normal *plus* membrane zone/fringe complex is most simply explained by proposing that this trait is normally specified by the absent *mt*⁺ locus. This inference is supported by the present work, for we show that the *imp-1* mutation selectively affects the production of a normal *plus* fringe, and we have shown previously (10) that the *imp-1* mutation maps to the *mt*⁺ locus.

Supported by grants from the National Institutes of Health and by Fellowship #HD-05886 to P. A. Detmers.

REFERENCES

1. Bergman, K., U. W. Goodenough, D. A. Goodenough, J. Jawitz, and H. Martin. 1975. Gametic differentiation in *Chlamydomonas reinhardtii*. II. Flagellar membranes and the agglutination reaction. *J. Cell Biol.* 67:606–622.
2. Cavalier-Smith, T. 1975. Electron and light microscopy of gametogenesis and gamete fusion in *Chlamydomonas reinhardtii*. *Protoplasma.* 86:1–18.
3. Detmers, P. A. and U. W. Goodenough. 1980. Actin in the *Chlamydomonas* mating type' mating structure. *J. Cell Biol.* 87(2, Pt.2): 220*a* (Abstr.).
4. Ebersold, W. T., R. P. Levine, E. E. Levine, and M. A. Olmsted. 1962. Linkage maps of *Chlamydomonas reinhardi*. *Genetics.* 47:531–543.
5. Forest, C. L., and R. K. Togasaki. 1975. Selection for conditional gametogenesis in *Chlamydomonas reinhardi*. *Proc. Natl. Acad. Sci. U. S. A.* 72:3652–3655.
6. Forest, C. L., D. A. Goodenough, and U. W. Goodenough. 1978. Flagellar membrane agglutination and sexual signaling in the conditional *gam-1* mutant of *Chlamydomonas*. *J. Cell Biol.* 79:74–84.
7. Friedman, L., A. L. Colwin, and L. H. Colwin. 1968. Fine structural aspects of fertilization in *Chlamydomonas reinhardi*. *J. Cell Sci.* 3:115–128.
8. Goodenough, U. W. 1977. Mating interactions in *Chlamydomonas*. *In:* Microbial Interactions. Receptors and Recognition, Series B. J. L. Reissig, editor. Vol. 3. Chapman and Hall, London. 323–350.
9. Goodenough, U. W., W. S. Adair, E. Caligor, C. L. Forest, J. L. Hoffman, D. A. M. Mesland, and S. Spath. 1980. Membrane-membrane and membrane-ligand interactions in *Chlamydomonas* mating. *In:* Membrane-Membrane Interactions, N. B. Gilula, editor Raven Press, New York 131–152.
10. Goodenough, U. W., C. Hwang, and H. Martin. 1976. Isolation and genetic analysis of mutant strains of *Chlamydomonas reinhardtii* defective in gametic differentiation. *Genetics.* 82:169–186.
11. Goodenough, U. W., C. J. Hwang, and A. J. Warren. 1978. Sex-limited expression of gene loci controlling flagellar membrane agglutination in the *Chlamydomonas* mating reaction. *Genetics.* 89:235–243.
12. Goodenough, U. W., and D. Jurivich. 1978. Tipping and mating-structure activation induced in *Chlamydomonas* gametes by flagellar membrane antisera. *J. Cell Biol.* 79:680–693.
13. Goodenough, U. W., and R. L. Weiss. 1975. Gametic differentiation in *Chlamydomonas reinhardtii*. III. Cell wall lysis and microfilament-associated mating structure activation in wild-type and mutant strains. *J. Cell Biol.* 67:623–637.

14. Hwang, C., B. C. Monk, and U. W. Goodenough. 1981. Linkage of mutations affecting *minus* flagellar membrane agglutinability to the *mt*$^-$ mating type locus of *Chlamydomonas*. Genetics. In press.
15. Johnson, U. G., and K. R. Porter. 1968. Fine structure of cell division in *Chlamydomonas reinhardi:* basal bodies and microtubules. *J. Cell Biol.* 38:403–425.
16. Martin, N. C., and U. W. Goodenough. 1975. Gametic differentiation in *Chlamydomonas reinhardtii.* I. Production of gametes and their fine structure. *J. Cell Biol.* 67:587–605.
17. Matagne, R., R. Deltour, and R. Ledoux. 1979. Somatic fusion between cell wall mutants of *Chlamydomonas reinhardi. Nature* (*Lond.*). 278:344–346.
18. Mesland, D. A. M., J. L. Hoffman, E. Caligor, and U. W. Goodenough. 1980. Flagellar tip activation stimulated by membrane adhesions in *Chlamydomonas* gametes. *J. Cell Biol.* 84:599–617.
19. Richardson, C. D., A. Scheid, and P. W. Choppin. 1980. Specific inhibition of paramyxovirus and myxovirus replication by oligopeptides with amino acid sequences similar to those at the N-termini of the F_1 or HA_2 viral polypeptides. *Virology.* 105:205–222.
20. Sager, R., and Z. Ramainis. 1974. Mutations that alter the transmission of chloroplast genes in *Chlamydomonas. Proc. Natl. Acad. Sci. U. S. A.* 71:4698–4702.
21. Smith, G. M., and D. C. Regnery. 1950. Inheritance of sexuality in *Chlamydomonas reinhardi. Proc. Natl. Acad. Sci. U. S. A.* 36:246–248.
22. Snell, W. J. 1976. Mating in *Chlamydomonas:* a system for the study of specific cell adhesion. I. Ultrastructural and electrophoretic analyses of flagellar surface components involved in adhesion. *J. Cell Biol.* 68:48–69.
23. Triemer, R. E., and R. M. Brown. 1975. Fertilization in *Chlamydomonas reinhardi*, with special reference to the structure, development, and fate of the choanoid body. *Protoplasma.* 85:99–107.
24. Weiss, R. L., D. A. Goodenough, and U. W. Goodenough. 1977. Membrane differentiations at sites specialized for cell fusion. *J. Cell Biol.* 72:144–160.
25. Wiese, L. 1965. On sexual agglutination and mating-type substances (gamones) in isogamous heterothallic Chlamdomonads. I. Evidence of the identity of the gamones with surface components responsible for sexual flagellar contact. *J. Phycol.* 1:46–54.